A Simplified Numerical Framework for Evaluating Post-Earthquake Settlements of Rc Frames

Ernesto Grande[1,2,*], Maura Imbimbo[1,2], Valentina Tomei[1,2] and Mehmet Yigitbas[1,2]

[1]*Department of Civil and Mechanical Engineering, University of Cassino and Southern Lazio, Italy*

[2]*European University of Technology EUt+, Viale dell'Università, 03043, Campus Folcara, Cassino, European Union, Italy*

Abstract: This paper investigates the response of reinforced concrete (RC) frames to post-earthquake settlements, a critical condition for structures founded on liquefiable soils. A simplified numerical framework is proposed to account for the interaction between seismic-induced damage and subsequent ground deformations through a sequential analysis procedure. The approach combines nonlinear dynamic analyses and a simplified static-based method for estimating the residual post-earthquake configuration, followed by the application of settlements through an idealized compression-only support model. This element simulates a support that can transfer compressive forces while losing contact under tension, thus allowing settlement to develop without artificially constraining uplift conditions. Moreover, the residual configuration refers to the permanent deformed state of the structure at the end of the seismic action, including accumulated inelastic deformations and damage. The results show that seismic damage significantly affects the initial stiffness and load redistribution capacity during settlement, leading to increased settlement demands for a given load level. However, the ultimate settlement capacity remains largely unchanged when the collapse mechanism is not modified. For higher seismic intensities, a reduction in ultimate settlement capacity is observed, depending on the damage distribution and structural configuration. The comparison between dynamic and simplified static procedures demonstrates that the latter can capture the main features of the response with acceptable accuracy, providing a computationally efficient tool for preliminary assessments and parametric studies.

Keywords: Settlements, earthquake, time-history analysis, pushover analysis, RC frames, F.E. model.

1. INTRODUCTION

Soil liquefaction happens when the soil suddenly and temporarily loses much of its strength and stiffness, and it is one of the most serious effects of earthquakes [1–3]. Damage to buildings with shallow foundations due to post-liquefaction settlements comes from both the earthquake shaking and the liquefaction itself. During strong earthquakes, large inelastic deformations can occur and cause permanent displacements. These permanent damages can significantly affect how buildings respond to settlements [4]. Therefore, it is essential to assess seismic damage and post-earthquake settlements together to obtain realistic estimates of vulnerability for reinforced concrete (RC) structures in liquefaction-prone areas.

The literature includes many studies on soil-structure interaction [5–7] and on how foundation settlements affect the vulnerability of RC structures. In particular, although predicting building damage from differential settlements is difficult, there are empirical methods [8], approaches based on structural engineering principles ([9,10]) and numerical modelling methods [11–14]. For numerical methods, finite element analyses are usually done in two ways: uncoupled analyses, where the soil and the structure are studied separately, and the soil settlement profile is imposed on the structure as a load; coupled analyses, where soil-structure interaction is modelled explicitly.

In this coupled assessment process, a main uncertainty is the combined effect of ground shaking and liquefaction. During strong earthquakes, structures can suffer large inelastic deformations that lead to permanent residual displacements. Although seismic performance is often measured by peak deformation demand, large permanent lateral deformations at the end of the earthquake (i.e., residual displacements) may have a crucial role when evaluating how a building will respond in later events.

Estimating seismic residual displacements is challenging because they usually show greater variability between records than peak inelastic displacements ([15,16]). Many studies specifically address the evaluation of residual displacements after earthquakes. For example, in [17] it was shown that the ratio between post-yield and initial stiffness largely controls the amplitude of residual drifts by proposing formulas useful for a fast estimation of residual displacements of RC frames after earthquakes. Extensions to multi-degree-of-freedom frames were also carried out by confirming that residual drifts depend on how damage is distributed and how stiffness degrades [18,19].

Despite these advances, recent studies have further emphasized the importance of accounting for the interaction between liquefaction-induced ground

*Address correspondence to this author at the Department of Civil and Mechanical Engineering; University of Cassino and Southern Lazio; Italy;
E-mail: e.grande@unicas.it

Received on 10-03-2026 Accepted on 14-04-2026 Published on 17-04-2026

E-ISSN: 3083-3590/26

deformations and structural response within a consistent framework. In particular, recent contributions have investigated the response of structures subjected to liquefaction-induced settlements and ground deformations, highlighting the role of soil–structure interaction and foundation compliance in modifying both seismic demand and post-earthquake performance [20–23].

At the same time, advances in performance-based earthquake engineering have improved the understanding and prediction of residual displacements and damage states in reinforced concrete (RC) frames, including simplified approaches capable of estimating post-seismic residual configurations with reduced computational effort [24–26].

However, despite these developments, existing approaches generally treat seismic damage and settlement effects either independently or through computationally demanding fully coupled models, without explicitly linking the residual structural configuration induced by earthquakes to the subsequent settlement response within a unified and efficient analysis framework.

The proposed framework is intended to provide a computationally efficient yet physically consistent tool for evaluating how damage accumulated during seismic events influences the subsequent settlement response, with particular focus on stiffness degradation, load redistribution mechanisms, and ultimate settlement capacity.

Starting from a two-story reference frame in both Weak-Beam (WB) and Strong-Beam (SB) schemes and three levels of vertical load, the method first estimates the residual configuration after the seismic action. Then it applies post-seismic settlements via a uniaxial spring model representing the soil's loss of stiffness under compression-only behaviour. The approach is improved by simplifying the evaluation of seismic residual displacements: instead of time history analyses, it introduces a recent method based on nonlinear static analyses proposed by the Authors.

The results show the role of different key parameters in the interaction between damage accumulated during the earthquake and the subsequent settlements. Moreover they underline the reliability of the simplified procedure based on static analyses.

To better clarify the positioning of the present study with respect to existing contributions, it is worth emphasizing that the proposed framework does not aim to reproduce the full complexity of soil–structure interaction phenomena through advanced geotechnical modelling. Instead, the objective is to develop a simplified and computationally efficient structural analysis procedure capable of capturing the interaction between residual seismic damage and subsequent settlements in a consistent and physically interpretable manner.

Within this context, the novelty of the study lies in three main aspects. First, a sequential analysis workflow is defined, in which the structural state resulting from vertical loading and seismic action is explicitly transferred to a subsequent settlement phase, allowing the role of residual damage to be directly quantified. Second, the soil is represented through an idealized compression-only uniaxial spring, not intended to model the full soil response, but to provide a controlled and consistent way to impose settlements while preserving equilibrium and compatibility within the structural system. Third, the framework incorporates a simplified nonlinear static-based procedure for estimating the residual post-earthquake configuration of the frame, enabling a direct comparison with time-history analyses and significantly reducing the computational effort.

In this sense, the proposed approach differs from existing studies, which are typically focused either on fully coupled soil–structure interaction models or on independent assessments of seismic and settlement effects, without explicitly linking the residual structural configuration to the subsequent settlement response within a unified framework.

In particular, while fully coupled soil–structure interaction models aim at reproducing the detailed constitutive behavior of the soil, they often involve high computational cost and require advanced geotechnical characterization. On the other hand, uncoupled approaches typically neglect the influence of residual seismic damage on the subsequent settlement response, treating the two phenomena independently.

The proposed framework provides an intermediate solution, in which the structural response is analyzed through a sequential procedure that explicitly accounts for the residual state induced by seismic loading, while maintaining a simplified and computationally efficient representation of soil compliance.

2. MATERIALS AND METHODS

The approach proposed in this study aims to investigate the combined effects of seismic actions and subsequent settlements, replicating typical conditions associated with soil liquefaction phenomena. To this end, a simplified two-story reinforced concrete (RC)

frame was selected as a reference structure. Two different structural configurations were considered to evaluate how specific design choices influence the settlement response following an earthquake.

The selection of a two-story, single-bay frame is intentional and is aimed at providing a controlled benchmark configuration in which the interaction between seismic-induced damage and post-earthquake settlements can be clearly isolated and interpreted. In more complex structural systems, additional mechanisms such as redundancy, load redistribution among multiple vertical elements, and spatial variability of response may obscure the interpretation of the underlying phenomena. The adopted simplified geometry therefore allows focusing on the fundamental mechanics governing the sequential response, while limiting the influence of higher-order effects.

The first configuration adopts a weak beam–strong column mechanism (WB), wherein beams are designed to yield before columns in case of seismic actions, following capacity design principles for ductile seismic response. The second configuration features a strong beam–weak column mechanism, in which columns yield prior to beams, representing a less desirable but still observed scenario in existing structures. These two schemes reflect contrasting behaviors toward seismic actions in terms of seismic strength, ductility, and expected damage accumulation at the end of the earthquake.

For both configurations, three different levels of vertical loading, comprising dead and live loads, were applied to explore the influence of axial force in the columns on the response of frame toward post-earthquake settlements.

The overall analysis workflow adopted in this study is illustrated in Figure **1**, which can be interpreted as a flowchart of the proposed sequential procedure. The framework is organized into three main phases, each corresponding to a distinct structural state and loading condition.

Indeed, the analysis procedure follows the three sequential phases illustrated in Figure **1**:

i. Vertical loading phase: the frame is analyzed under gravity loads with fixed base conditions, establishing the initial stress and deformation state;

ii. Seismic phase: starting from the previous state, a nonlinear dynamic (time-history) analysis is performed under fixed base conditions;

iii. Post-earthquake settlement phase: the boundary conditions are modified by releasing vertical constraints and introducing a compression-only spring element, through which settlements are imposed via a prescribed vertical displacement.

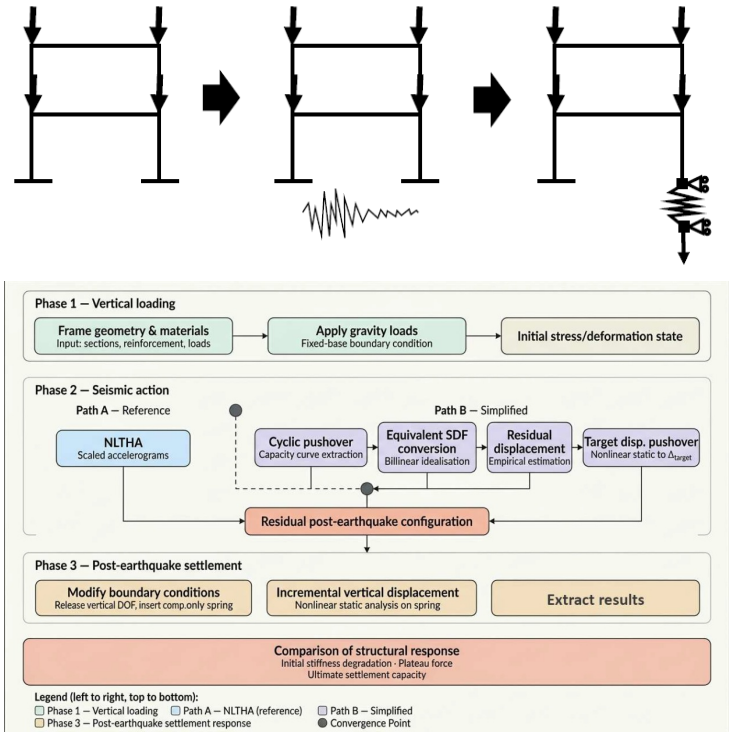

Figure 1: Schematization of the subsequent phases of analysis: load conditions and boundary constraints of frame.

The adopted spring element is not intended to reproduce the full constitutive behavior of the soil, particularly under liquefaction conditions. Instead, it represents an idealized and concentrated formulation of vertical support compliance, introduced to simulate the effects of imposed settlements within a sequential structural analysis framework. In this context, the spring is used as a simplified mechanical device that allows transferring a prescribed vertical displacement to the structure while maintaining equilibrium and compatibility conditions. The compression-only behavior reflects the physical condition of soil, which can sustain compressive stresses but cannot transmit tensile forces once detachment occurs. This modelling choice is consistent with the objective of the present study, which is not to simulate the generation of settlements from soil constitutive laws, but rather to investigate the structural response of RC frames subjected to post-seismic settlements, explicitly accounting for the residual damage accumulated during the earthquake phase. However, this simplified representation introduces several limitations that must be acknowledged. The model does not account for the nonlinear and cyclic degradation of soil stiffness, nor for the evolution of excess pore pressure during liquefaction. Furthermore, the interaction between vertical and horizontal soil response is neglected, as well as possible foundation rotation, uplift, or spatial variability of settlements. The soil is therefore represented as a local vertical compliance without any distributed or continuum description. As a consequence, the proposed approach should be interpreted as a structural assessment tool aimed at capturing the interaction between residual seismic damage and imposed settlements in a consistent and computationally efficient manner, rather than as a detailed soil–structure interaction model.

The numerical simulations were carried out using the software OpenSees [27]. To ensure continuity between the sequential phases (vertical loading - seismic response - post-earthquake settlement), a custom script was developed in MATLAB [28]. This script allows tracking the structural state at the end of each phase and updates the boundary and load conditions accordingly for the next stage of analysis.

The analysis of results focuses both on local damage, evaluated in terms of level of curvature at cross-sections and on global settlement response, expressed through force–settlement curves. These curves represent the relationship between the vertical load transferred to the soil and the imposed settlement, providing a global measure of the structural response under foundation displacement.

In the following, the force–settlement response is described in terms of the axial force transmitted to the soil, denoted as N, and the imposed vertical displacement, denoted as δ. For normalization purposes, the axial force is expressed with respect to the initial value under vertical loading, N_v.

Here, the “force” corresponds to the vertical reaction transmitted to the soil (i.e., the axial force in the column adjacent to the spring), and the “settlement” is the imposed vertical displacement at the free end of the spring (i.e., the node connected to the column by the spring). These curves reveal two distinct behavioral phases: an initial phase where internal forces are redistributed among frame members, followed by the formation of a mechanism where the frame continues to deform under increasing settlement without significant change in transmitted force. Both phases eventually halt with structural collapse, marked by the attainment of ultimate curvature in beams or columns.

The present study is part of a broader research activity conducted by the authors on the vulnerability assessment of existing structures to seismic-induced phenomena, such as soil liquefaction. Within this framework, the authors have previously proposed efficient simplified procedures for estimating the residual state of low-rise RC frames by employing nonlinear static analyses instead of computationally demanding time-history simulations. Then, in continuation with the previous study, the modeling approach developed in the present work for simulating the post-earthquake settlement response is also employed to validate a hybrid procedure, in which the residual state of the frame at the end of the earthquake is estimated through the simplified method proposed in [29], and the subsequent response to settlements is analyzed using the modeling approach presented herein. This validation aims to assess the accuracy and applicability of the combined method, which significantly reduces computational effort while preserving the ability to capture key aspects of structural behavior under coupled seismic and post-seismic actions.

3. CASE STUDIES

The case studies selected to validate the proposed approach consist of a simple two-story, one-bay reinforced concrete frame, as illustrated in Figure **2**. Two structural configurations have been considered. The first configuration, referred to as the Weak Beam (WB) scheme, features beams and columns with identical cross-sectional dimensions and reinforcement details, consistent with the one-story frame analyzed in [4,30]. Specifically, both beams and columns have square cross-sections measuring 350 × 350 mm. The columns are reinforced with 8 longitudinal steel bars of 22 mm diameter, while the beams are reinforced with 4

bars of 14 mm diameter, placed symmetrically at the top and bottom of the section (see Figure **2**). This configuration leads to a flexural capacity of the beams lower than that of the columns converging at the same joint, thus promoting a weak beam-strong column seismic mechanism.

The second configuration, referred to as the Strong Beam (SB) scheme, differs from the WB configuration only in the design of the beams. To achieve beam-column joints where the beams are stronger than the columns, the height of the beam cross-section is increased to 700 mm, and the longitudinal reinforcement is increased to 4 bars of 22 mm diameter, placed at the top and bottom of the section.

For both schemes, three different levels of vertical load (including dead and live loads) have been considered, assuming the same value at each story. The first load level leads to a total vertical force at the base equal to 40 kN and corresponds to the reference configurations WB and SB. The second load level corresponds to a total vertical force at the base equal to 20 kN, and the related configurations are denoted as WB-Nhalf and SB-Nhalf. The third load level produces a total vertical force at the base equal to 80 kN, with the respective schemes referred to as WB-Ntwice and SB-Ntwice.

In all configurations, concrete with strength class C28/35 and reinforcing steel grade B450C have been adopted.

Furthermore, the same value of lumped mass, equal to 41.76 Ns²/mm has been assumed for all models.

4. MODELING APPROACH AND PERFORMED ANALYSES

Numerical simulations were carried out using the OpenSees software [27], employing the same finite element modeling framework and material constitutive relationships previously assumed in [4] for the analysis of a single-story frame. That prior study validated the adopted modeling strategy and parameter choices through comparison with experimental data.

This aspect is particularly relevant in the present study, as the reliability of the sequential analysis framework depends on the accuracy of the adopted structural model in capturing nonlinear response, damage accumulation, and stiffness degradation. Therefore, the previously validated modelling strategy is here adopted as a consistent and reliable basis for the subsequent analyses, ensuring that the observed response trends are not influenced by modelling inconsistencies but rather reflect the effects of the imposed loading sequence and boundary condition variations.

The adopted finite element model follows a distributed plasticity formulation, wherein the cross-sections of beam and column elements are subdivided into fibers, each associated with a nonlinear material response based on its respective constituent material. The cross-section is divided into a confined concrete core, an unconfined cover region, and discrete longitudinal reinforcement bars. Although the same type of constitutive law is assigned to both the core and cover concrete, different strength and strain limits are used to capture the effects of confinement within the core region.

The concrete behavior is described using the uniaxial Concrete04 material model from the OpenSees library, which is derived from the formulation proposed by [31]. This model incorporates tensile strength, stiffness degradation, and post-peak softening. The reinforcing steel is modeled using Steel02, also from the OpenSees library, which features a bilinear stress–strain response with

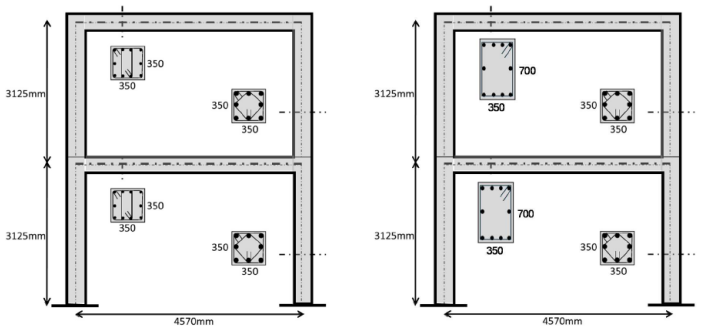

WB scheme

Beams:350x350mm

4ϕ14mm (top)-4ϕ14mm (bottom)

Columns:350x350mm - 8 ϕ 22mm

SB scheme

Beams:350x700mm

4ϕ22mm (top)-4ϕ22mm (bottom)

Columns:350x350mm - 8 ϕ 22mm

Figure 2: Reference RC-frame cases.

Table 1: Parameters of the Uniaxial Material Model Concrete04 Selected for Concrete Material and the Uniaxial Material Model Steel02 Selected for Steel Material of Reinforcement

	fc[MPa]	ε_c	ε_{cu}	E_c [MPa]	f_{ct} [MPa]	ε_t	β
beam - cover	-37.05	-0.002	-0.0035	32588	1.98	0.00004	0.1
column – cover	-37.05	-0.002	-0.0035	32588	1.98	0.00004	0.1
beam - core	-39.17	-0.0023	-0.0181	32989	2.08	0.00004	0.1
column – core	-38.59	-0.0022	-0.0141	32989	2.05	0.00004	0.1
f_c: compressive strength							
ε_c: strain at the maximum strength							
ε_{cu}: strain at crashing strength							
E_c: initial stiffness							
f_{ct}: maximum tensile strength							
ε_{ct}: ultimate tensile strain							
β: parameter defining residual stress							
		f_y [MPa]	E_0 [MPa]	b	R_0	c_{R1}	c_{R2}
beam – columns bars		521	210000	0.03	18	0.925	0.15
f_y: yield strength							
E_0: initial elastic tangent							
b: strain hardening							
R_0; c_{R1}; c_{R2}: parameters controlling the transition from elastic to plastic branches (here set equal to the average of recommended values)							

kinematic and isotropic hardening. A perfect bond between reinforcement and concrete is assumed, thereby neglecting possible slip effects. The specific parameters adopted for both material models are listed in Table **1**. These were derived from mechanical characterization tests reported in [32], and further supplemented by national code provisions.

Additional details can be found in [33] and [4], where similar modeling approaches were adopted. As for the structural discretization, beam and column elements were represented using force-based frame elements (ForceBeamColumn) with Gauss–Lobatto integration, as implemented in OpenSees. Each member was modeled using two elements, with two integration points for the columns and three for the beams. As noted in [33], this choice reflects a trade-off between numerical efficiency and the ability to capture the experimental behavior observed in the tests conducted by [32].

Regarding the numerical analyses, a preliminary set of simulations was carried out to evaluate the response of the considered case studies to seismic actions and, separately, to settlement effects.

In particular, for the seismic actions, pushover analyses were performed on a frame model with fixed base, applying horizontal forces distributed along the height proportionally to the shape of the first vibration mode. The modal analysis of the frame in the two configurations, WB and SB, resulted in a first vibration period of 0.51 s and 0.43 s, respectively, and in a ratio between the second and first components of the first mode shape equal to 2.065 and 1.716, respectively.

The settlement effects, on the other hand, were investigated by applying vertical loads only and, subsequently, imposing a progressively increasing vertical displacement at the free end of the spring element.

In both cases, the analyses were stopped when the ultimate curvature was reached in a beam or column section.

Regarding the adopted values of the ultimate curvature, it is estimated in this work using simplified expressions that combine the ultimate compressive strain of concrete with the ultimate tensile strain of reinforcing steel. For both beams and columns, the following general expression is adopted:

$$\phi_u = \frac{\varepsilon_{cu}+\varepsilon_{su}}{h-c} \quad \text{eq (1)}$$

where:

ε_{cu} is the ultimate strain of concrete (typically assumed as 0.018 for confined concrete);

ε_{su} is the ultimate tensile strain of reinforcing steel (often taken as 0.04 for ductile steel);

h is the overall section height;

c is the concrete cover to the reinforcement.

Eqn. 1 assumes a linear distribution of strains across the section at ultimate conditions and that failure occurs due to the simultaneous attainment of the ultimate strains in concrete and steel at opposite extreme fibers. The approach is consistent with the idealized strain profiles used in performance-based design and in displacement-based assessment methods, as outlined in [34].

After these preliminary analyses, the combined effects of seismic action and settlement were studied using the procedure proposed in this work. As shown in the scheme in Figure **1**, the first phase consisted of analyzing the frame with fixed base under vertical loads only. In the second phase, starting from the deformed state obtained at the end of the first step and still assuming fixed base conditions, a nonlinear dynamic (time-history) analysis was performed using one of the seven selected spectrum-compatible accelerograms. In the final phase, the vertical restraints at the base of the columns and at the end of the spring were removed, and a vertical displacement was applied to the spring's end node. This displacement was gradually increased while performing a nonlinear static analysis. The procedure was repeated for all the accounted accelerograms.

The accelerograms used for the dynamic analyses are the same accounted in [4].

In particular, a set of seven spectrum-compatible accelerograms was adopted, selected to match the target elastic response spectrum corresponding to a return period of 2475 years for the reference site conditions. The selection was carried out using the REXEL software [35] considering the following parameters: site location in Mirandola, Italy (LON: 11.1 – LAT: 44.9); equivalent damping ratio of 5%; return period of 2475 years; and EC8 Site Class C (Figure **3**), and ensuring compatibility in terms of spectral shape within the period range relevant for the fundamental modes of the considered structures. The adopted records are not intended to represent a statistically exhaustive sample of ground motions, but rather a consistent set of spectrum-compatible accelerograms suitable for comparative analysis. In this context, the number of records is aligned with common practice in nonlinear dynamic analyses, where a limited but representative set is used to capture record-to-record variability while maintaining computational efficiency. Record-to-record variability is explicitly considered in the interpretation of results. In particular, the response of the structure is evaluated for each individual accelerogram, and the corresponding dispersion is illustrated in the presented figures through the set of curves associated with different records. In addition, average response trends are used as reference quantities, especially for comparison with the simplified static-based procedure. For parametric analyses, additional scaling of the selected records is performed by modifying the peak ground acceleration (PGA), in a manner consistent with incremental dynamic analysis approaches. This allows exploring different levels of seismic intensity and corresponding damage states, while preserving the spectral characteristics of the original records. It is worth noting that the adopted approach focuses on the structural consequences of seismic damage rather than on a probabilistic seismic assessment. Therefore, the selected ground motion set is used to generate physically consistent damage scenarios, rather than to derive statistically robust demand estimates.

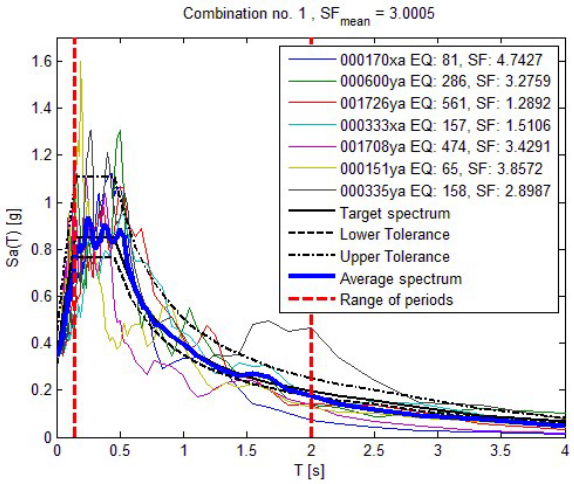

Figure 3: Spectra of the accounted accelerograms (thin lines); average spectrum of selected accelerogram (thick line); target spectrum from the code (thin continuous black line).

In the final part of the paper, is presented a set of simulations carried out by integrating in the phases of analysis the simplified procedure proposed by [4], specifically employed for evaluating the residual damage of reinforced concrete frames after an earthquake through a set of nonlinear static analyses rather than a more computationally demanding time-history analysis. Further details on this approach are provided in the second part of the paper.

5. RESULTS

The results obtained from the analyses are presented below, both in terms of local behavior, by examining the forces and deformations in the beam and column sections marked in Figure **4**, and in terms of global response. For the pushover analyses, the typical Base Shear vs. Top Displacement curves are shown, while in the case of settlements, the results are presented as curves that relate the force transmitted from the structure to the soil with the corresponding imposed settlement.

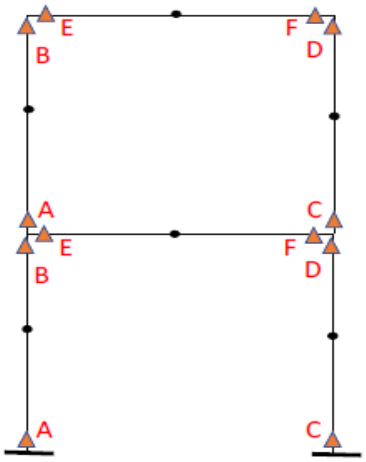

Figure 4: Scheme of the frame with marked sections.

5.1. Post-Earthquake Effects on Settlement Response

5.1.1. Seismic Response (Pushover Analyses)

The results of the pushover analyses are shown in Figure **5** as Base Shear vs. Top Displacement curves. These curves clearly highlight the different behavior between the frame with weak beams and the one with strong beams. In particular, this difference is especially evident in terms of peak load, while the ultimate displacement corresponding to the attainment of the ultimate curvature is almost the same in both cases. The influence of the axial force level in the columns on the overall response appears to be limited. It is almost negligible in the WB case, while it becomes more noticeable in the SB case.

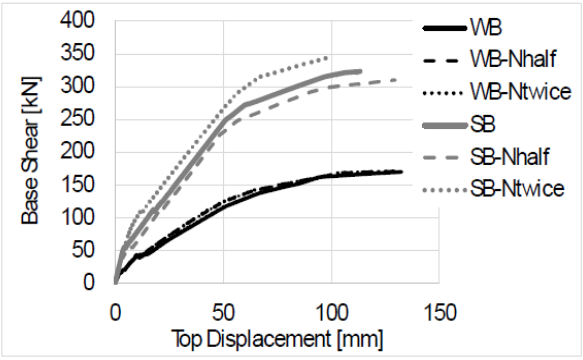

Figure 5: Capacity curves derived from pushover analysis.

The analysis of the local behavior at the ends of beams and columns (Figure **6** to Figure **11**) shows that, in the WB configuration, the yield curvature is reached at both ends of the beams on the first and second stories, and also at the base of the first-story columns. The ultimate curvature is reached in the first-story beam. This behavior remains the same regardless of the axial force level in the columns.

In contrast, in the SB configuration, the yield curvature is reached at the ends of both columns on the first story, leading to a typical soft-story mechanism. The beams, on the other hand, remain in the elastic range, and the ultimate curvature is reached in the columns.

These results represent a preliminary evaluation useful for understanding the seismic behavior of the considered frame configurations in the absence of settlement effects.

5.1.2. Settlement-Only Response

Regarding the response of the frames to settlement only, the results in terms of global response are shown in Figure **12**. The curves represent the axial force in the spring placed between the two nodes at the base of the column, one at the column's end and the other at the spring's end where the settlement is applied. This force, called *Force*, is normalized with respect to the axial force in the first-story column when no settlement is applied (*Nv*), i.e. the axial force of the base column in the phase of application of vertical loads only, and it is plotted against the applied settlement (*Settlement*). According to the model used in this study, the axial force in the spring is equal to the axial force in the column (in case of compression), which represents the force that the structure transfers to the soil. In the first part of the response, the curves show an almost linear decrease in the load transferred to the soil. This is due to shear forces in the beams, which redistribute the axial loads to other parts of the structure in the elastic stage. When a mechanism forms due to the yielding of beam or column sections, the load transferred to the soil cannot decrease further, and the curve reaches a sort of plateau. The plateau corresponds to the stage in which a collapse mechanism has formed and further settlement occurs with limited variation of the transmitted force.

Figure **12a** compares the behavior of the two configurations, WB and SB, under the same level of vertical loading (i.e., the same initial axial force in the columns before applying the settlement). The two schemes show a similar trend, both in the first stage, where the axial force in the spring decreases with increasing settlement, and in the point where the maximum reduction of force is reached, corresponding to the formation of a collapse mechanism in the frame.

For the WB configuration, the analysis of the moment-curvature diagrams of the beam and column end sections (Figure **13**) shows a final mechanism characterized by the yielding of both ends of the first-story beam and the yielding of the base sections of both first-story columns. The shear forces in the first-story beam increase until the yield moment is reached, while in the second-story beam the shear increases until the base of the first-story columns yields

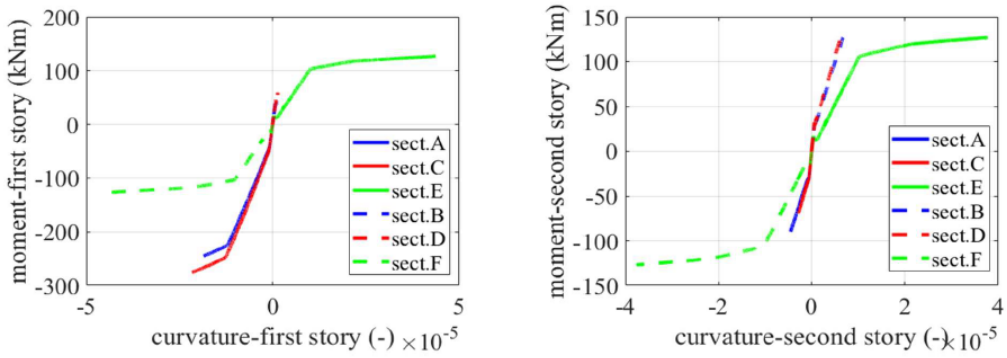

Figure 6: Pushover analysis: sections behavior for WB scheme with fixed base.

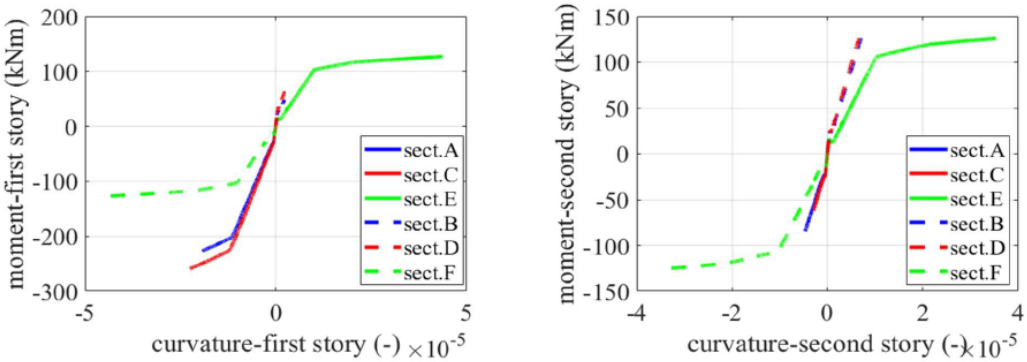

Figure 7: Pushover analysis: sections behavior for WB-Nhalf scheme with fixed base.

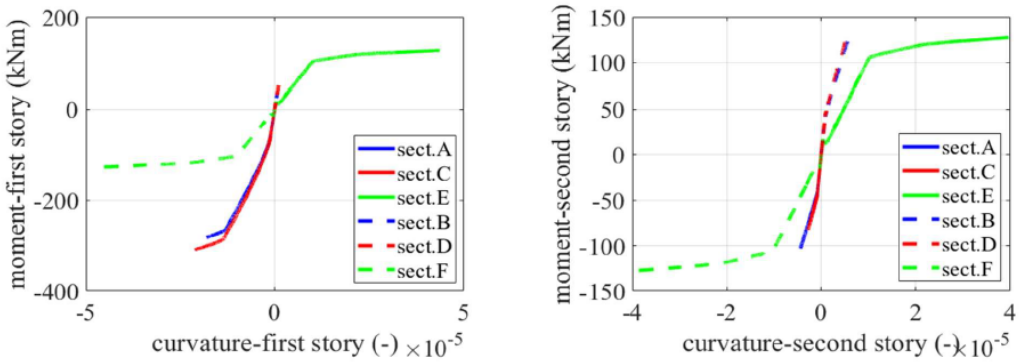

Figure 8: Pushover analysis: sections behavior for WB-Ntwice scheme with fixed base.

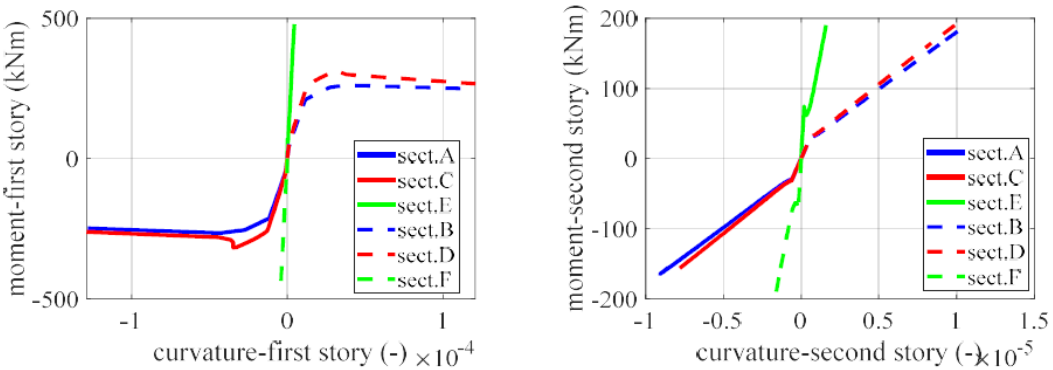

Figure 9: Pushover analysis: sections behavior for SB scheme with fixed base.

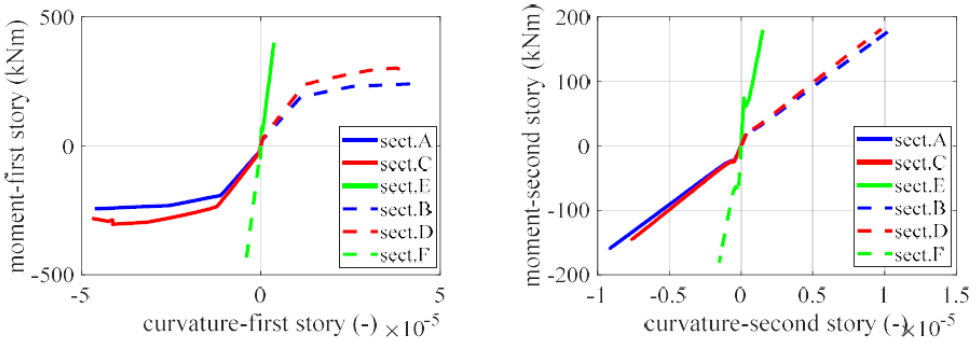

Figure 10: Pushover analysis: sections behavior for SB-Nhalf scheme with fixed base.

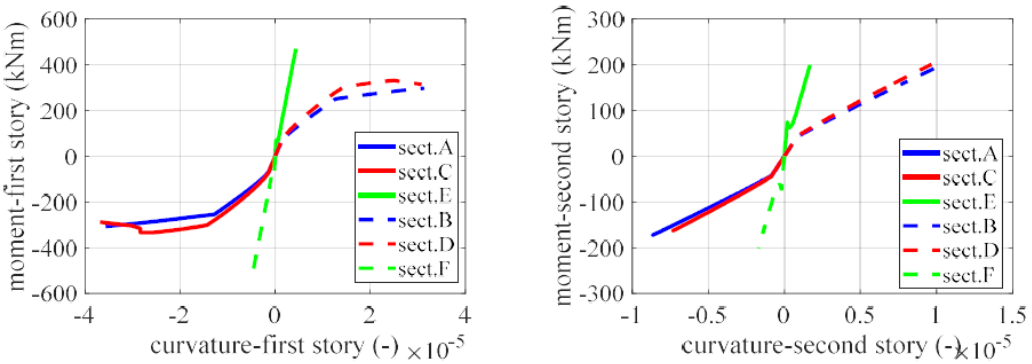

Figure 11: Pushover analysis: sections behavior for SB-Ntwice scheme with fixed base.

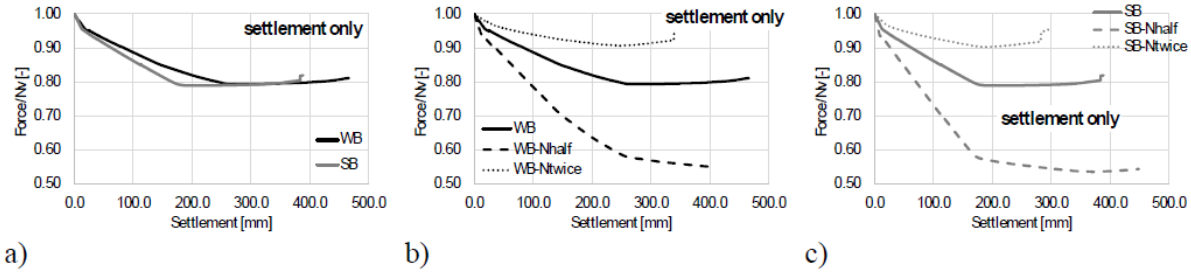

Figure 12: Nonlinear static analyses: results obtained by applying settlements without seismic actions.

(Figure **13**). From simple equilibrium considerations, it can be assessed that the axial force in the spring at the plateau corresponds almost to the axial force in the case without settlement, minus the shear force in the right end section of the beams at the settlement corresponding to the plateau.

In the SB configuration, the beams remain elastic while both ends of the first-story columns yield. In this case, it was observed that the shear force in the first-story beam was approximately equal to the shear developed in the WB scheme (Figure **14**). As a result, the axial force in the spring at the plateau is similar to that observed in the WB case.

As expected, varying the vertical loads (and thus the initial axial force in the columns) causes a proportional change in both the initial slope and the plateau of the curves, since the final collapse mechanism remains unchanged (see Figure **12b**, **12c**).

The observations from this first set of analyses provide a basis for analyzing the post-earthquake effects on settlement response of RC frames.

The results discussed above provide a reference baseline for interpreting the influence of seismic-induced damage on the subsequent settlement response.

5.2. Combined Seismic and Post-Earthquake Settlement Response

The following results illustrate the structural response when the effects of seismic damage and

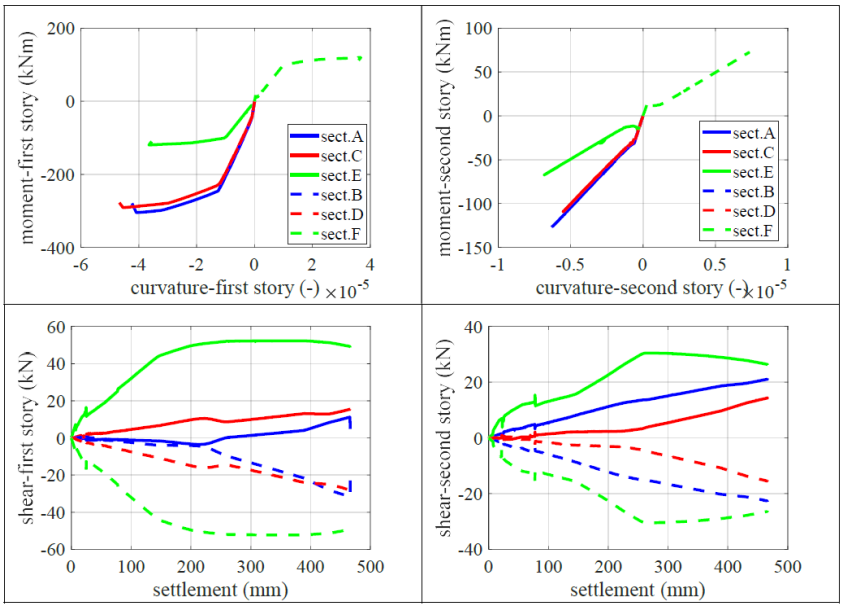

Figure 13: Moment-curvature of beam and column end sections (upper); shear forces (bottom): WB scheme.

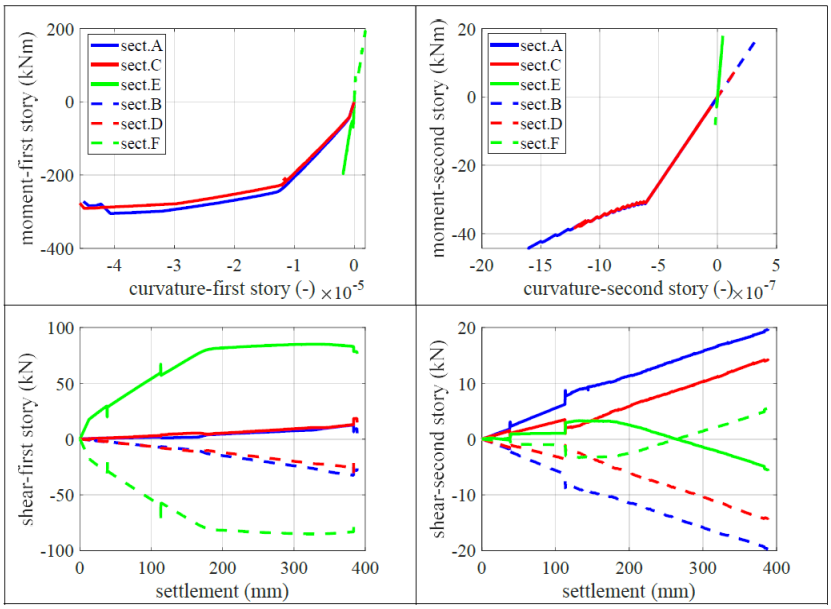

Figure 14: Moment-curvature of beam and column end sections (upper); shear forces (bottom): SB scheme.

subsequent settlements are considered in a sequential and coupled manner.

The effects of post-earthquake damage on the settlement response are analyzed by following the sequence of analysis phases shown in Figure **1**.

The corresponding results are illustrated in Figure **15**, again in the form of curves representing the axial force in the spring element located between the two nodes at the base of the column, one at the column's end, and the other at the spring's end where the settlement is applied. Each graph shows both the reference curve (thick black line), obtained by considering settlement only, and the curves obtained by including the effects of the earthquake (thin grey lines).

From the plots, it is clear that in all analyzed cases, the influence of earthquake-induced damage is particularly visible in the initial part of the curve, where the frame can still redistribute internal forces as settlement increases. On the other hand, the final response, namely the reduction in force and the settlement value at which the ultimate section curvature is reached, is not significantly influenced by the earthquake. This is because the collapse mechanism remains essentially the same of the case with settlement only.

However, for the same force transferred to the ground, the earthquake-damaged frame shows a larger settlement. In other words, after experiencing seismic damage, the frame tends to transfer higher axial forces to the ground as the imposed settlement increases. As

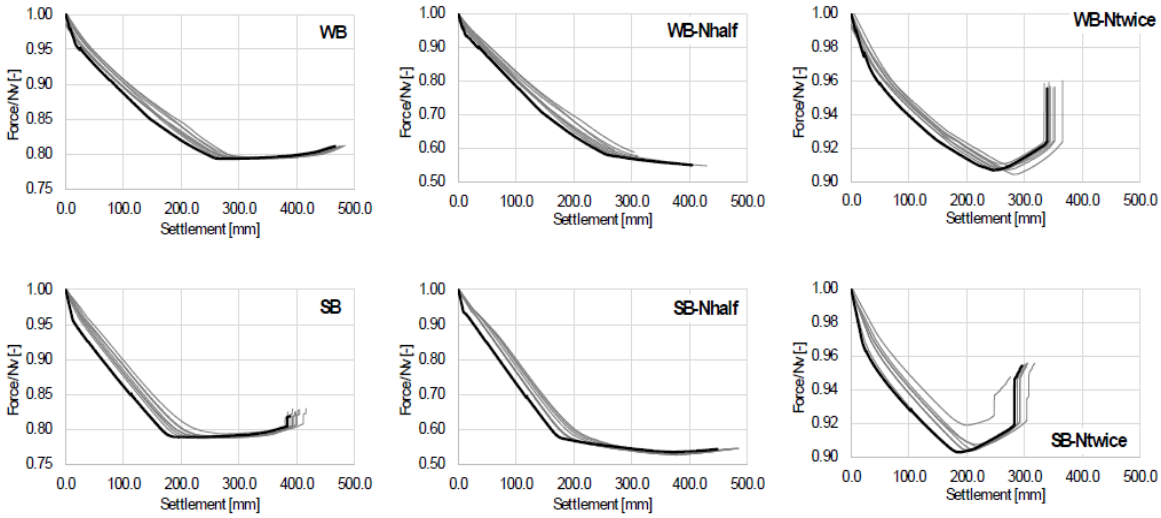

Figure 15: Force-Settlement curves: settlement only (thick black line), earthquake and settlement (thin grey lines).

a result, the damaged frame reaches the plateau of the curve at slightly lower force values, which highlights the reduction in vertical load-bearing capacity due to the previous seismic event.

Despite this, the results do not show a significant difference in the final settlement values, that is, the settlement at which the ultimate curvature is reached in beams or columns does not change substantially.

It is clear that the results strongly depend on the level of residual damage in the reinforced concrete (RC) frames caused by the earthquake.

Figure **16** shows the same set of force–settlement curves already presented in Figure **15**, but obtained by scaling the input accelerograms by a factor of two in order to simulate stronger seismic events and consequently higher levels of structural damage. As in the previous figure, each sub-plot displays both the reference response due to settlement only (thick black line) and the responses accounting for the combined effects of earthquake and settlement (thin grey lines).

Compared to the unscaled case, the results clearly highlight the intensification of the effects of earthquake-induced damage. In particular, two distinct consequences can be observed. First, during the initial phase of settlement, the redistribution of internal forces becomes more sensitive to the altered stiffness and damage conditions of the frame, leading to a more scattered behavior among the grey curves. Second, and more importantly, a noticeable shift is observed in the final branch of the curves, with some configurations showing a reduction in the ultimate load-bearing capacity and an earlier attainment of the collapse mechanism, i.e., the ultimate curvature in critical sections.

This evidence confirms that higher levels of residual damage due to stronger seismic inputs significantly affect both the redistribution capacity of the structure

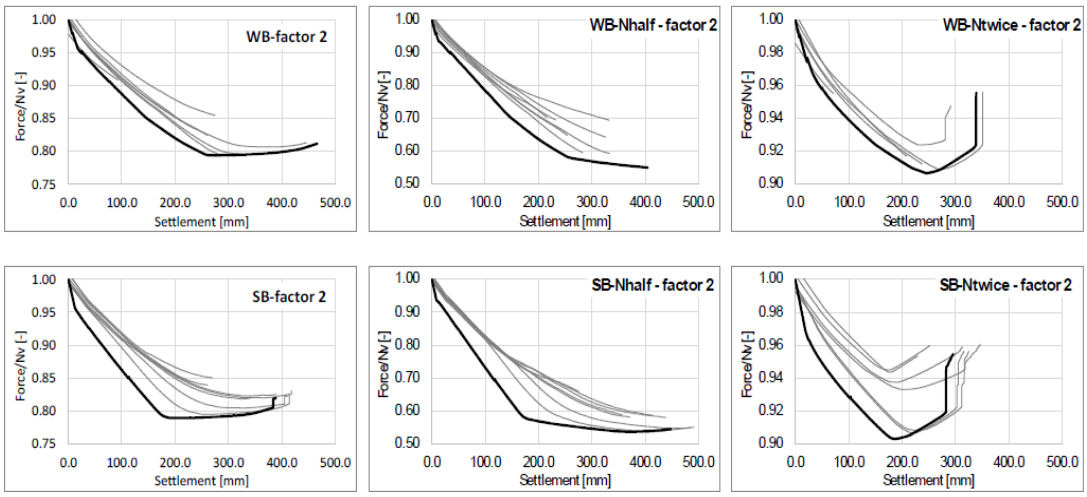

Figure 16: Force–settlement curves obtained from accelerograms scaled by a factor of two: settlement only (thick black line), earthquake and settlement (thin grey lines).

and its residual strength during the settlement phase. The ultimate settlement is governed by whether the seismic damage alters the failure mechanism activated by settlement, or whether it leads to an earlier attainment of the ultimate curvature due to the prior degradation of structural capacity. Therefore, the key factor is not just the settlement level itself, but the interaction between the accumulated seismic damage and the collapse mode triggered during the post-earthquake settlement.

From an engineering perspective, the obtained results highlight that the effect of post-earthquake damage on settlement response is not uniform across the different phases of structural behavior.

In the initial stage of settlement, the response is strongly governed by the residual stiffness and by the ability of the frame to redistribute internal forces. Seismic damage, by reducing stiffness and altering the distribution of plastic hinges, limits this redistribution capacity, leading to a steeper degradation of the force–settlement response. This effect is particularly relevant for serviceability and early damage conditions, where even moderate settlements may induce higher stress concentrations in already damaged members.

On the other hand, the ultimate settlement capacity is primarily controlled by the collapse mechanism activated in the structure. When the seismic damage does not significantly modify this mechanism, the ultimate settlement remains almost unchanged. Conversely, when the damage alters the hierarchy of resisting elements or leads to premature attainment of ultimate curvature in critical sections, a reduction in settlement capacity is observed. This explains the different trends obtained for increasing PGA levels and for different structural configurations.

The comparison between WB and SB schemes further highlights the role of structural design in controlling post-earthquake settlement response. Frames designed according to capacity design principles (WB) tend to accumulate damage in beams, which may lead to a more distributed degradation of stiffness and a higher sensitivity to settlement in the early stages. In contrast, SB configurations, characterized by column-dominated mechanisms, show a more localized damage pattern, which affects the global response differently.

From a practical standpoint, these findings indicate that neglecting the residual damage induced by seismic actions may lead to non-conservative

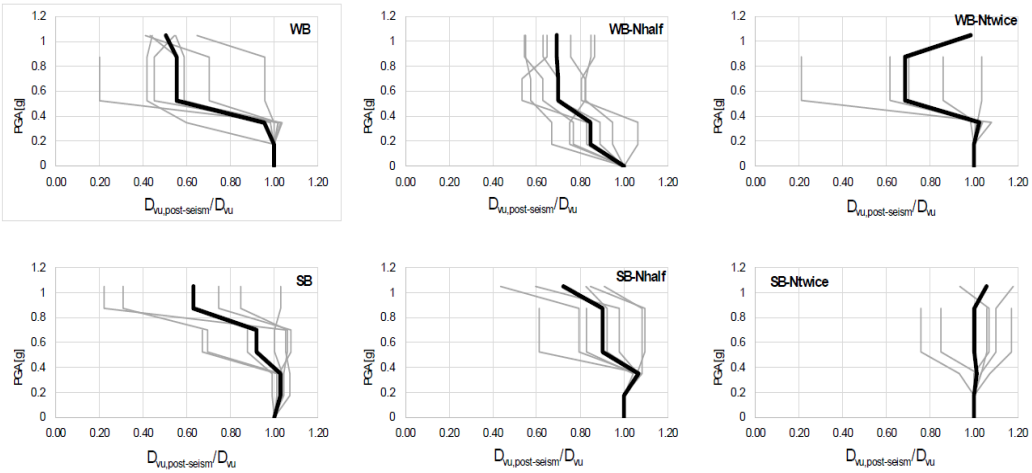

Figure 17: Normalized ultimate settlement after the earthquake vs. PGA curves: results related to individual accelerograms (grey lines); average trend (thick black lines).

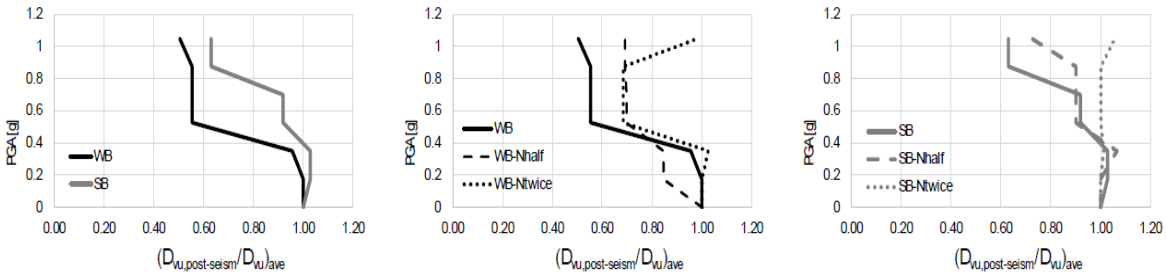

Figure 18: Average normalized ultimate settlement after the earthquake vs. PGA curves.

assessments of structural performance under post-earthquake settlements, particularly in terms of stiffness degradation and load redistribution capacity. Therefore, simplified assessment procedures that explicitly account for the residual structural state, such as the one proposed in this study, may provide a valuable tool for preliminary evaluations, large-scale assessments, and parametric analyses.

These findings are consistent with previous studies highlighting the importance of residual seismic displacements in structural response (e.g., [17–19]), while extending their application to the analysis of post-earthquake settlement effects. Unlike most existing approaches, which either consider settlements independently or rely on fully coupled soil–structure interaction models, the present study provides a simplified framework in which the residual structural configuration is directly incorporated into the settlement analysis.

To further investigate this aspect, additional analyses were carried out using the same set of spectrum-compatible accelerograms, but scaling the peak ground acceleration (PGA), like the common Incremental Dynamic Analyses performed in case of seismic analysis.

The results are shown in Figure **17**, where the relationship between PGA (ranging from 0, meaning no seismic action, up to 1.05g) and the ultimate settlement after the earthquake, $D_{vu,post-seism}$, is reported. The ultimate settlement after the earthquake is normalized with respect to the value obtained in the absence of seismic action, D_{vu}.

The grey curves represent the results for each of the seven accelerograms, while the thick black curve is the average trend. In some cases, the curves stop before reaching the accounted PGA value because the residual damage in the structural members due to seismic action was higher than the ultimate value of section curvature here considered.

The results highlight a clear trend of decreasing ultimate settlement capacity with increasing PGA. This reduction is influenced by both the structural configuration and the axial load level in the columns. Specifically, the Weak Beam (WB) configuration appears more sensitive to seismic damage than the Strong Beam (SB) scheme. This difference is more clearly visualized in Figure **18**, which compares the average normalized curves for all configurations. The figure illustrates how higher axial loads and weaker beam-column hierarchies worsen the loss of settlement capacity following seismic events.

6. SIMPLIFIED NONLINEAR STATIC-BASED EVALUATION OF POST-SEISMIC SETTLEMENT RESPONSE

In a recent research study, the authors proposed a simplified method for evaluating the residual post-seismic response of low-rise RC frames [29]. This method consists of a multi-phase procedure that uses the monotonic seismic response of RC frames to estimate the residual displacements after an earthquake, avoiding the need for Time History Analyses.

Specifically, the proposed method is developed through a four-phase process that combines pushover analysis with empirical relationships derived for single-degree-of-freedom (SDF) systems (refer to the preliminary steps for evaluating the residual deformed shape with top displacement D_{res} shown in Figure **19**). First, a pushover analysis with a loading and unloading cycle is performed to determine the static residual displacement at the top of the frame, $D_{stat,res}$. During the loading cycle, the maximum expected displacement

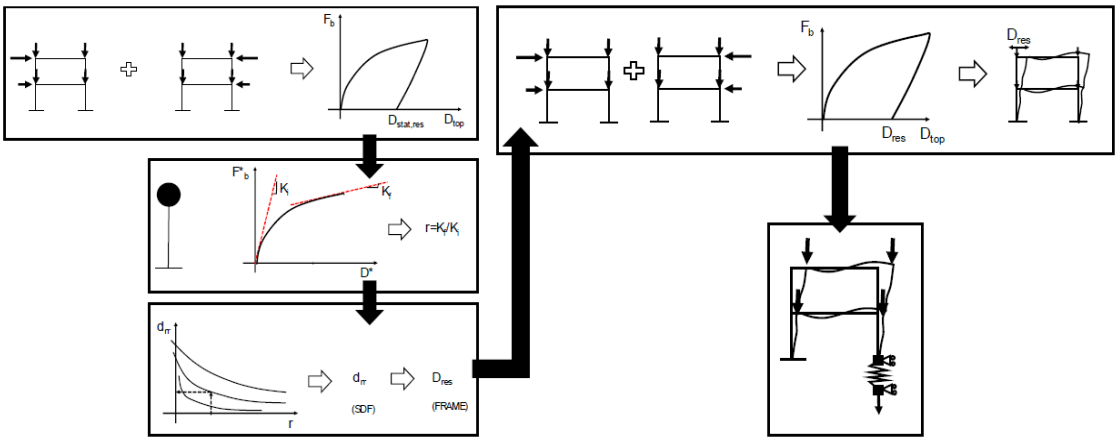

Figure 19: Combined procedure based on preliminary nonlinear static analyses for evaluating the residual post-earthquake status of frame and the subsequent application of settlements.

related to the design seismic action is attained. Then, the unloading cycle is performed until obtaining a null value of the base shear of the frame. The capacity curve obtained during the loading cycle is transformed into the one of the equivalent SDF system in order to calculate the ratio between the initial (elastic) stiffness and the final (post-elastic) stiffness (this ratio is called *r*). Using this parameter, along with the static residual top displacement obtained at the end of the unloading cycle, the residual top displacement is estimated directly by applying the empirical formulas proposed by [17]. Based on the estimated residual top displacement D_{res}, a further loading/unloading pushover analysis (set in order to obtain at the end of the unloading cycle just the estimated value of the residual top displacement) is performed to evaluate the residual interstory displacements along the frame height and, then, the residual damaged configuration of the frame.

The results presented in [29] showed a good reliability of this approach in estimating the residual post-earthquake damaged configuration of low-rise RC-frames.

In the present study, this approach is used to replace the phase dedicated to evaluating the post-earthquake damage configuration of the structure. In other words, it is used for the estimation of post-seismic effects on the settlement response of RC frames without carrying out time-history analyses. According to the procedure shown in Figure **19**, once the residual post-earthquake damaged configuration of frames is estimated using the static method proposed by [4], the settlement is then applied using the modeling strategy presented in this work, i.e. by varying the boundary constraints and applying a vertical displacement to the end joint of the spring.

The results are shown in Figure **20** for both the WB and SB schemes, once again in the form of force–settlement curves that represent the axial force in the nonlinear spring element placed between the bottom of the column and the point where the settlement is imposed. These are the same types of curves already discussed in Figure **15**, allowing a direct comparison of the results obtained with the two different procedures. In each plot, the thin grey lines correspond to the curves obtained by applying the procedure described in Figure **1**, which includes the effect of seismic damage before the application of the settlement by using time history analysis. The thick black line shows the response of the system when only the settlement is applied, without considering any prior seismic action. The red dotted curve, labeled AV, represents the results deduced by accounting for the approach proposed in [4] where the average law proposed by McRae was selected (for further details, see the study by [4]).

In this context, the comparison between the results obtained through nonlinear time-history analyses and those derived from the simplified static-based procedure can be interpreted as a benchmark-oriented validation of the proposed framework. In particular, the time-history analyses are assumed as a reference solution, while the simplified approach is assessed in terms of its ability to reproduce the main features of the structural response under post-earthquake settlement conditions.

The results of this comparison show that, for both structural schemes, the curve deduced by introducing the static approach is generally in good agreement with the average trend of the curves obtained from time-history analyses.

To provide a quantitative assessment of the agreement between the two approaches, the comparison is further evaluated in terms of normalized error measures. In particular, the percentage difference between the static-based prediction and the average dynamic response is computed at selected points of the force–settlement curves.

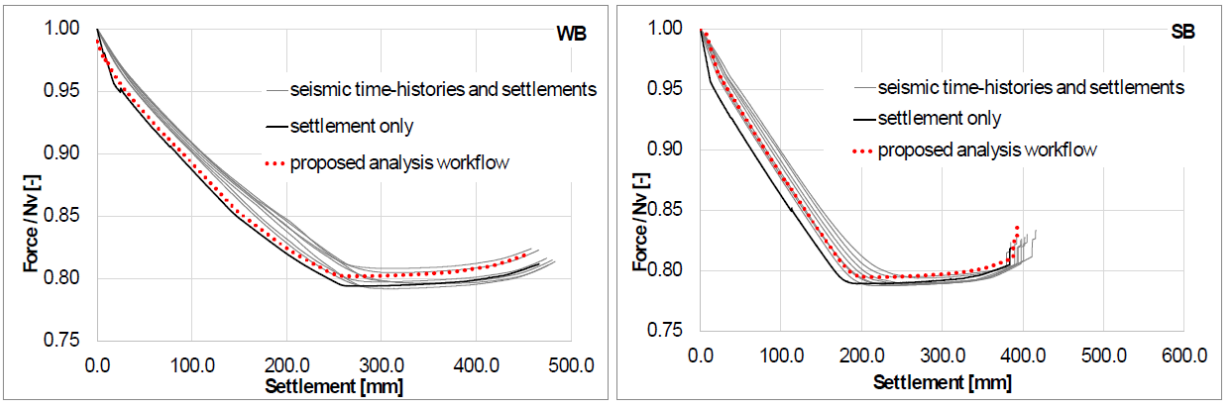

Figure 20: Force–settlement curves obtained for the simplified procedure: comparison with the approach based on static analysis.

Three key response parameters are considered: (i) the initial slope of the curve, representing the stiffness in the early stage of settlement; (ii) the plateau force, corresponding to the load level associated with the formation of the collapse mechanism; and (iii) the ultimate settlement, defined as the displacement at which the ultimate curvature is reached.

The results show that the simplified static-based approach reproduces the initial stiffness with deviations generally on the order of 5–12%. The plateau force is captured with very good accuracy, with differences typically within 2–3%. Slightly larger discrepancies are observed in the intermediate settlement range, particularly for the WB configuration, where the static method tends to slightly overestimate the residual capacity. However, the ultimate settlement is predicted with good accuracy, with differences generally remaining within approximately 2–5% of the values obtained from time-history analyses.

These results confirm that, despite its simplified nature, the proposed static-based procedure provides a quantitatively reliable approximation of the average structural response, especially with regard to the key parameters governing the post-earthquake settlement behavior.

In the WB configuration, the AV curve slightly overestimates the residual capacity in the intermediate settlement range but remains consistent with the average behavior. In the SB configuration, the AV curve aligns more closely with the central part of the grey curve set, especially at larger settlements. This confirms that the simplified approach here proposed provides a reliable support for evaluating the effects of combined seismic damage and subsequent settlements.

7. CONCLUSIONS

The study presented a simplified coupled soil–structure numerical procedure to evaluate the influence of earthquake-induced damage on the subsequent settlement response of RC frames in liquefaction-prone scenarios. Considering a two-story, one-bay RC frame as reference, two structural schemes and three axial load levels were considered. The two accounted structural schemes were finalized to reproduce two different typical seismic responses of RC frames toward seismic actions: the weak-beam/ strong-column mechanism and strong-beam/ weak-column mechanism. The three levels of axial loads were imposed to explore how different gravity-load ratios modify the post-seismic settlement capacity.

The results obtained from the numerical analyses underlined that the implemented workflow in OpenSees, combining vertical preloading, nonlinear dynamic (time-history) analysis, and post-earthquake settlement analysis via a uniaxial spring model, underlined the influence of post-earthquake damages on the response toward settlement response. The results obtained from the numerical analyses clearly quantify the influence of earthquake-induced damage on the subsequent settlement response of RC frames. For the considered seismic intensity level (PGA ≈ 0.35g), the degradation of the initial stiffness of the force–settlement response is evident in all configurations, with reductions in stiffness associated with residual damage and altered redistribution capacity. In contrast, the ultimate settlement capacity is only marginally affected when the collapse mechanism remains unchanged.

A more pronounced effect is observed at higher seismic intensities. Incremental dynamic analyses show that increasing PGA leads to a progressive reduction in ultimate settlement capacity, with reductions that become significant for higher damage levels and are more pronounced in the WB configuration. This confirms that the impact of seismic damage on settlement response is strongly dependent on both the intensity of the seismic input and the resulting damage distribution.

The comparison between nonlinear time-history analyses and the simplified static-based procedure shows that the latter is able to reproduce the main features of the structural response with acceptable accuracy. In particular, the simplified approach estimates the initial stiffness with deviations on the order of 10–15%, the plateau force with differences typically below 10%, and the ultimate settlement within approximately 5–10% of the values obtained from dynamic analyses.

From an engineering perspective, these results indicate that neglecting residual seismic damage may lead to non-conservative assessments of structural response under post-earthquake settlements, especially in the initial stages where stiffness degradation governs the behavior. At the same time, the proposed simplified framework provides a computationally efficient tool capable of capturing the key mechanisms of the problem, making it suitable for preliminary assessments, parametric studies, and large-scale applications where full nonlinear dynamic analyses would be impractical.

Incremental dynamic analyses revealed that in-creasing PGA reduces the ultimate settlement capacity, with more pronounced effects in the WB scheme.

This further underlines that seismic damage can play a dual role particularly depending on whether it

alters the collapse mechanism activated by settlement. Indeed, in some cases, the damage reduces the settlement capacity, causing the structure to reach ultimate curvature at a lower imposed settlement; in others, the damage reduces the axial force capacity, leading to earlier attainment of collapse for the same level of settlement, without necessarily changing the deformation mode. This variability depends on the extent and distribution of seismic-induced damage and its interaction with the failure mechanisms triggered by ground settlement. Then, the results underline the importance of accounting not only for the residual stiffness and strength degradation but also for potential changes in the governing failure mechanism.

The integration of a recent nonlinear static procedure (pushover-based residual displacement estimation with MacRae-type empirical relationships) to replace time-history analyses by static analyses led to force–settlement curves in good agreement with the ones derived by dynamic-based results. In particular, for WB frames, the static method slightly overestimates residual capacity in intermediate settlement ranges (i.e., gives slightly unconservative estimates), whereas for SB frames the match is excellent across the settlement domain. This confirmed that the hybrid static approach can significantly reduce computational effort while preserving acceptable accuracy, especially for preliminary assessments or parametric studies.

In conclusions, post-earthquake settlements can substantially increase demand on already damaged RC frames. Therefore, analysis frameworks that couple seismic effects and subsequent soil deformations (e.g., liquefaction-induced settlements) are crucial for realistic vulnerability assessment of low-rise structures in liquefaction-prone areas.

It should be noted that the validation provided in this study is limited to a benchmark comparison between nonlinear dynamic analyses and a simplified static-based procedure within a consistent structural modelling framework. The proposed approach does not aim to validate soil constitutive behavior or to reproduce the full complexity of soil–structure interaction phenomena.

Furthermore, although the analyses are carried out on a simplified two-story, single-bay frame, this configuration is intentionally adopted as a controlled benchmark to isolate the fundamental mechanisms governing the interaction between residual seismic damage and post-earthquake settlements. While the quantitative results are specific to the analyzed case studies, the proposed sequential framework and modelling strategy are general and can be extended to more complex structural systems.

In multi-bay and multi-story frames, additional mechanisms such as redistribution of axial forces among multiple columns, alternative collapse modes, torsional effects, and spatial variability of settlements may influence the response. However, the key trends identified in this study, particularly the role of residual seismic damage in modifying stiffness, load redistribution capacity, and settlement response, are expected to remain relevant.

Future developments will focus on extending the proposed framework to more complex structural configurations and more refined soil–structure interaction models, as well as on further validation against experimental or high-fidelity numerical benchmarks.

AKNOWLEDGEMENTS

This work was supported by the Italian Ministry of University and Research (MUR) under the PNRR framework, Mission 4, Component 2, Investment 1.3, funded by the European Union – NextGenerationEU.

In particular, it was developed as part of the project “Sustainable Approaches For Earthquake Resistant Rehabilitation Solutions for Built Environment” (SAFER-REBUILT), funded through the “Bando a Cascata” call issued by the University of Bari Aldo Moro (Rector's Decree no. 3658, 12/10/2023).

This initiative is a component of the broader “Multi-Risk Science for Resilient Communities under a Changing Climate” (RETURN) project (Code PE00000005, CUP H93C22000610002), specifically under Spoke VS3 titled “Earthquakes and Volcanoes”.

AUTHOR CONTRIBUTIONS: CREDIT

Ernesto Grande: Conceptualization, Data curation, Formal analysis, Methodology, Software, Supervision, Validation, Visualization, Writing – original draft, Writing – review and editing. Maura Imbimbo: Data curation, Methodology, Supervision, Validation, Writing – review and editing. Valentina Tomei: Data curation, Methodology, Supervision, Validation, Writing – review and editing. Mehmet Yigitbas: Data curation, Methodology, Visualization, Validation, Writing – review and editing.

REFERENCES

[1] Karamitros DK, Bouckovalas GD, Chaloulos YK. Seismic settlements of shallow foundations on liquefiable soil with a clay crust. Soil Dyn Earthq Eng 2013. https://doi.org/10.1016/j.soildyn.2012.11.012

[2] Bray JD, Dashti S. Liquefaction-induced building movements. Bull Earthq Eng 2014. https://doi.org/10.1007/s10518-014-9619-8

[3] Lirer S, Chiaradonna A, Mele L. Soil liquefaction: from mechanisms to effects on the built environment. Rivista Italiana di Geotecnica 2020.

[4] Grande E, Lirer S, Milani G. Simple approach to evaluate the influence of seismic residual displacements on post-liquefaction settlements of RC-frames. Structures 2022; 37: 411-25. https://doi.org/10.1016/j.istruc.2022.01.022

[5] Nasab MSE, Chun S, Kim J. Soil-structure interaction effect on seismic retrofit of a soft first-story structure. Structures 2021; 32: 1553-64. https://doi.org/10.1016/j.istruc.2021.03.105

[6] Hamidia M, Shokrollahi N, Nasrolahi M. Soil-structure interaction effects on the seismic collapse capacity of steel moment-resisting frame buildings. Structures 2021; 32: 1331-45. https://doi.org/10.1016/j.istruc.2021.03.068

[7] Jafarieh AH, Ghannad MA. Seismic performance of nonlinear soil-structure systems located on soft soil considering foundation uplifting and soil yielding. Structures 2020; 28: 973-82. https://doi.org/10.1016/j.istruc.2020.09.046

[8] Skempton AW, Macdonald DH. The allowable settlements of buildings. Proc Inst Civ Eng 1956. https://doi.org/10.1680/ipeds.1956.12202

[9] Bird JF, Crowley H, Pinho R, Bommer JJ. Assessment of building response to liquefaction-induced differential ground deformation. Bull New Zeal Soc Earthq Eng 2005. https://doi.org/10.5459/bnzsee.38.4.215-234

[10] Burland JB, Wroth CP. Settlement of buildings and associated damage. Settl. Struct. Proc. Conf. Br. Geotech. Soc., 1974.

[11] Burd HJ, Houlsby GT, Augarde CE, Lill G. Modelling tunnelling-induced settlement of masonry buildings. Proc Inst Civ Eng Geotech Eng 2000. https://doi.org/10.1680/geng.2000.143.1.17

[12] Negulescu C, Foerster E. Parametric studies and quantitative assessment of the vulnerability of a RC frame building exposed to differential settlements. Nat Hazards Earth Syst Sci 2010. https://doi.org/10.5194/nhess-10-1781-2010

[13] Alessandri C, Garutti M, Mallardo V, Milani G. Crack patterns induced by foundation settlements: Integrated analysis on a renaissance masonry palace in Italy. Int J Archit Herit 2015. https://doi.org/10.1080/15583058.2014.951795

[14] Tiberti S, Grillanda N, Mallardo V, Milani G. A Genetic Algorithm adaptive homogeneous approach for evaluating settlement-induced cracks in masonry walls. Eng Struct 2020. https://doi.org/10.1016/j.engstruct.2020.111073

[15] Bojórquez E, Ruiz-García J. Residual drift demands in moment-resisting steel frames subjected to narrow-band earthquake ground motions. Earthq Eng Struct Dyn 2013; 42: 1583-98. https://doi.org/10.1002/eqe.2288

[16] Ruiz-García J, Miranda E. Residual displacement ratios for assessment of existing structures. Earthq Eng Struct Dyn 2006; 35: 315-36. https://doi.org/10.1002/eqe.523

[17] Macrae GA, Kawashima K. Post-earthquake residual displacements of bilinear oscillators. Earthq Eng Struct Dyn 1997. https://doi.org/10.1002/(SICI)1096-9845(199707)26:7<701::AID-EQE671>3.3.CO;2-9

[18] Pampanin S, Christopoulos C, Nigel Priestley MJ. Performance-based seismic response of frame structures including residual deformations. Part II: Multi-degree of freedom systems. J Earthq Eng 2003; 7: 119-47. https://doi.org/10.1080/13632460309350444

[19] Christopoulos C, Pampanin S, Nigel Priestley MJ. Performance-based seismic response of frame structures including residual deformations. Part I: Single-degree of freedom systems. J Earthq Eng 2003; 7: 97-118. https://doi.org/10.1080/13632460309350443

[20] Bray JD, Macedo J. 6th Ishihara lecture: Simplified procedure for estimating liquefaction-induced building settlement. Soil Dynamics and Earthquake Engineering 2017; 102: 215-231. https://doi.org/10.1016/j.soildyn.2017.08.026

[21] Dashti S, Bray JD. Numerical simulation of building response to liquefaction-induced ground deformation. Journal of Geotechnical and Geoenvironmental Engineering. 2013; 139(8): 1235-1249. https://doi.org/10.1061/(ASCE)GT.1943-5606.0000853

[22] Huseynli, S., De Luca, F., Karamitros, D. (2024). Review of Dynamic Soil-Structure Interaction Models. In: Kasimzade, A., Erdik, M., Kundu, T., Sucuoğlu, H., Clemente, P. (eds) Earthquake Resistant Design, Protection, and Performance Assessment in Earthquake Engineering. AERS 2023. Geotechnical, Geological and Earthquake Engineering, vol 54. Springer, Cham.

[23] Yilmaz D. Liquefaction, Building Response, and Seismic Settlement Mechanisms in the Adapazarı Basin. BSJ Eng. Sci. 2026; 9: 812-825. https://doi.org/10.34248/bsengineering.1863508

[24] Alwashali H, Maeda M, Ogata Y, Aizawa N, Tsurugai K. Residual seismic performance of damaged reinforced concrete walls. Eng Struct 2021; 243: 112673. https://doi.org/10.1016/j.engstruct.2021.112673

[25] Xiangyong N, Yuxin C, Jiaqi X. Residual deformation-based post-earthquake damage identification and residual capacity quantification of reinforced concrete columns using machine learning technology. Struct Health Monit 2026. https://doi.org/10.1177/13694332261433699

[26] Yigitbas M, Grande E, Imbimbo M. Sequential seismic and settlement analysis of reinforced concrete moment-resisting frames. Int J Earthq Eng 2025; 42(4). https://doi.org/10.65102/is202545

[27] Mazzoni S, McKenna F, Scott MH, Fenves GL. Open System for Earthquake Engineering Simulation (OpenSEES) user command-language manual. Pacific Earthq Eng Res Cent 2006.

[28] The Mathworks, Inc. MATLAB, Version 9.0 2016. MATLAB - MathWorks - MATLAB. WwwMathworksCom/Products/Matlab 2016.

[29] Grande E, Imbimbo M, Yigitbas M. A pushover-based simplified approach for predicting post-earthquake residual displacements in low-rise RC frames. Bulletin of Earthquake Engineering, Volume 23, Issue 11, pp. 4635-4656. https://doi.org/10.1007/s10518-025-02238-2

[30] Grande E, Milani G, Rotunno T, Fagone M. Numerical study of the effect of Post-Liquefaction settlements on the response of infilled RC-frames. Structures 2022. https://doi.org/10.1016/j.istruc.2022.09.035

[31] Popovics S. A numerical approach to the complete stress-strain curve of concrete. Cem Concr Res 1973. https://doi.org/10.1016/0008-8846(73)90096-3

[32] Morandi P, Hak S, Magenes G. Performance-based interpretation of in-plane cyclic tests on RC frames with strong masonry infills. Eng Struct 2018. https://doi.org/10.1016/j.engstruct.2017.11.058

[33] Bagnoli M, Grande E, Milani G. Numerical Study of the In-Plane Seismic Response of RC Infilled Frames. Constr Mater 2021; 1: 82-94. https://doi.org/10.3390/constrmater1010006

[34] Priestley MJN, Calvi GM, Kowalsky MJ. Displacement-Based Seismic Design of Structures. Pavia, Italy: IUSS Press; 2007.

[35] Iervolino I, Galasso C, Cosenza E. REXEL: Computer aided record selection for code-based seismic structural analysis. Bull Earthq Eng 2010; 8: 339-62. https://doi.org/10.1007/s10518-009-9146-1

https://doi.org/10.65904/3083-3590.2026.02.01